Relativistic quantum field theory approach to electron wave-packet tunneling: A fully causal process

M. Alkhateeb,[1] X. Gutierrez de la Cal,[2,3] M. Pons,[3,4] D. Sokolovski,[2,3,5] and A. Matzkin[6]
[1]*Research Unit Lasers and Spectroscopies (UR-LLS), naXys & NISM, University of Namur, Rue de Bruxelles 61, B-5000 Namur, Belgium*
[2]*Departmento de Química-Física, Universidad del País Vasco, UPV/EHU, 48940 Leioa, Spain*
[3]*EHU Quantum Center, Universidad del País Vasco, UPV/EHU, 48940 Leioa, Spain*
[4]*Departamento de Física Aplicada, Universidad del País Vasco, UPV/EHU, 48013 Bilbao, Spain*
[5]*IKERBASQUE, Basque Foundation for Science, E-48011 Bilbao, Spain*
[6]*Laboratoire de Physique Théorique et Modélisation, CNRS Unité 8089, CY Cergy Paris Université, 95302 Cergy-Pontoise cedex, France*

(Received 8 July 2024; revised 1 August 2024; accepted 15 January 2025; published 29 January 2025)

Recent results on electron tunneling across a potential barrier, inferred from observations or obtained from theoretical models, have suggested superluminal or instantaneous barrier traversal times. In this work we investigate relativistic wave-packet dynamics for an electron tunneling through a potential barrier employing space-time resolved solutions to relativistic quantum field theory (QFT) equations. We prove by linking the QFT property of microcausality to the wave-packet behavior that the tunneling dynamics is fully causal, precluding instantaneous or superluminal effects. We illustrate these results by performing numerical computations for an electron tunneling through a potential barrier for standard tunneling as well for Klein tunneling. In all cases (Klein tunneling or regular tunneling across a standard or a supercritical potential) the transmitted wave packet remains in the causal envelope of the propagator, even when its average position lies ahead of the average position of the corresponding freely propagated wave packet.

DOI: 10.1103/PhysRevA.111.012222

I. INTRODUCTION

Tunneling is one of the most intriguing quantum phenomena. Although tunneling underlies many important processes in about every area concerned by quantum physics (see, e.g., [1–7] for recent observations), its precise mechanism has remained controversial [8,9]. Despite experimental data coming from different areas, from strong field tunneling ionization [2,5,10–12] to cold atoms [3], neutron optics [13], or condensed matter [14], there seems to be no solution in view [15] to the tunneling time problem (the time spent by a particle inside the barrier) or, equivalently, the arrival time (whether a particle that tunnels through a barrier arrives earlier than a freely propagating particle). Indeed, due to the ambiguity of measuring time in quantum mechanics (there is no time operator in the standard formalism) any observed tunneling time will depend on the model employed to extract the time interval from the observed data.

In particular, experiments involving electron photoionization have reported results interpreted to indicate instantaneous tunneling times [2,5,10,11]. Such interpretations rely on models that intrinsically involve disputed approximations [16], generally employing a nonrelativistic and often semiclassical framework. Perhaps somewhat more surprisingly, several works based on a first-quantized relativistic framework [17–25] have concluded on the possibility of superluminal arrival times for electrons. Such superluminal transmissions could potentially bring serious issues with causality, even though it is sometimes asserted that these effects do not seem to lead to signaling [24]. Other investigations carried out within relativistic quantum mechanics have, on the contrary, not noted any superluminal effects at the level of the wave function [26–29].

In this work, we investigate the tunneling dynamics in a second-quantized framework. More specifically, we will employ a computational relativistic quantum field theory (QFT) approach in order to follow the space-time resolved dynamics of an electron tunneling through an electrostatic potential barrier represented by a background field. The electron is modeled as a wave packet initially defined on a compact support launched towards a potential barrier. We will prove that microcausality of the fermionic quantum field implies that the electron wave-packet density evolves causally, thereby ensuring the absence of any superluminal effects such as instantaneous tunneling times. The present method allows us to treat on the same footing different types of tunneling effects: the familiar one characterized by exponentially decaying waves inside the barrier, as well as Klein tunneling (with undamped oscillating waves in the barrier) for supercritical barriers (that is, barriers with a potential above the pair-production threshold).

We will begin by describing our theoretical approach in Sec. II, where we will define the wave packet as a second-quantized state and introduce the particle density operator from field operators obeying the Dirac equation. In Sec. III, we will see that microcausality holds for a fermionic field in the presence of a background potential and use this result to show that the tunneled wave-packet density is constrained by a causal evolution: the wave-packet density cannot leak outside the light cone. We will then give (Sec. IV) numerical results obtained with our QFT framework for three typical cases of tunneling, all cases displaying a causal behavior of the transmitted wave packet: standard tunneling through a nonradiating barrier (similar to the familiar tunneling situation known in nonrelativistic quantum mechanics), standard tunneling in the presence of a slightly radiating barrier (in which the transmitted wave packet is overshadowed by the electron density due to pair production), and Klein tunneling through a supercritical barrier, in which it is known that tunneling is mediated by pair production. We will discuss our results and conclude in Sec. V.

II. FRAMEWORK: QFT WITH A BACKGROUND POTENTIAL

A. First- and second-quantized evolutions

Our approach is based on a computational QFT framework [30], recently extended to treat particle scattering across a finite barrier [31] (see also [32,33] for related recent work). In this framework, an electron wave packet is described by a relativistic fermionic Dirac field, while the potential barrier on which the electron scatters will be described by a background "classical" field [34].

Let us first introduce the free Dirac Hamiltonian

$$H_0 = -i\hbar c\alpha_x\partial_x + \beta mc^2 \tag{1}$$

which has the eigenvalues $\pm|E_p| = \pm\sqrt{p^2c^2 + m^2c^4}$. α and β are the usual Dirac matrices (recall that in one spatial dimension, we can neglect spin flip and replace α_x and β by the Pauli matrices σ_1 and σ_3, respectively), m the electron mass, and c is the light velocity. The positive and negative energy solutions of Eq. (1) are, respectively, given by

$$v_p(x) = \begin{pmatrix} 1 \\ \frac{cp}{mc^2+E_p} \end{pmatrix} e^{ipx},$$
$$w_p(x) = \begin{pmatrix} 1 \\ \frac{cp}{mc^2-E_p} \end{pmatrix} e^{-ipx}. \tag{2}$$

The full first-quantized Hamiltonian

$$H = H_0 + V(x), \tag{3}$$

where $V(x)$ is a rectangularlike potential barrier. The Hamiltonian H generates a unitary evolution. Let U denote the unitary evolution operator of the full Hamiltonian with elements in the free Dirac basis given by

$$U_{v_k w_p}(t) \equiv \langle v_k|\exp(-iHt/\hbar)|w_p\rangle. \tag{4}$$

The second-quantized creation and annihilation operators for particle and antiparticles will be labeled $b_p^\dagger$ and b_p (for particles) and $d_p^\dagger$ and d_p (for antiparticles). Since we are dealing with a fermionic field the creation and annihilation operators anticommute, $[b_p, b_k^\dagger]_+ = [d_p, d_k^\dagger]_+ = \delta(p-k)$. $\|0\rangle\rangle$ defines the vacuum state, i.e., $b_p\|0\rangle\rangle = d_p\|0\rangle\rangle = 0$. We will be working as usual in the Heisenberg picture, so that these operators evolve according to [30]

$$b_p(t) = \int dk(U_{v_p v_k}(t)b_k(0) + U_{v_p w_k}(t)d_k^\dagger(0)), \tag{5}$$
$$d_p^\dagger(t) = \int dk(U_{w_p v_k}(t)b_k(0) + U_{w_p w_k}(t)d_k^\dagger(0)) \tag{6}$$

and their conjugates. Equations (5) and (6) give the QFT dynamics in terms of the first-quantized evolution operators. These equations will be seen to be the building blocks to carry out numerical computations.

B. Densities and field operators

For the purpose of investigating causality, we find it convenient for a matter of presentation to start from an initial wave packet perfectly localized within a compact spatial support. The second-quantized state describing this initial wave packet is written as

$$\|\chi\rangle\rangle = \int dp(g_+(p)b_p^\dagger(0) + g_-(p)d_p^\dagger(0))\|0\rangle\rangle, \tag{7}$$

where $g_\pm(p)$ are the wave-packet amplitudes in momentum space. As it is well known [35,36] a compactly localized state must contain both positive and negative energy components, hence the presence of both creation operators $b_p^\dagger$ and $d_p^\dagger$ in Eq. (7).

The particle density at any given time is given by the expectation value

$$\rho(t,x) = \langle\langle\chi\|\hat{\rho}(t,x)\|\chi\rangle\rangle, \tag{8}$$

where the density operator $\hat{\rho}(t,x)$ is defined by

$$\hat{\rho}(t,x) = \hat{\Phi}^\dagger(t,x)\hat{\Phi}(t,x). \tag{9}$$

Recall that in the absence of a wave packet, the density would be given instead by the vacuum expectation value $\langle\langle 0\|\hat{\rho}(t,x)\|0\rangle\rangle$.

$\hat{\Phi}(t,x)$ is the field operator. Since we are working with states having compact spatial support, we depart from the usual definition of the field operators and define them instead through [37]

$$\hat{\Phi}(t,x) = \int dp(\hat{b}_p(t)v_p(x) + \hat{d}_p(t)w_p(x)) \tag{10}$$

and its Hermitian conjugate

$$\hat{\Phi}^\dagger(t,x) = \int dp(\hat{b}_p^\dagger(t)v_p^\dagger(x) + \hat{d}_p^\dagger(t)w_p^\dagger(x)). \tag{11}$$

Indeed the standard field operators [36] cannot describe a compactly localized state. We stress, however, that the results described in this work do not depend on taking an initial compact state; the proofs given below also hold for the standard field operators and the quantum states of pure positive energy presenting infinite tails. The field operators (10) and (11) obey an important property: the equal-time anticommutator is given by

$$[\hat{\Phi}^\dagger(t,x'), \hat{\Phi}(t,x)]_+ = \delta(x'-x) \tag{12}$$

just like the familiar field operators of the free Dirac field [38]. Equation (12) is proved in Appendix A.

The computation of the density proceeds by pluging in Eqs. (9), (7) and (10), (11) into Eq. (8).

This gives

$$\rho(t,x) = \langle\langle 0\| \int dp(g_+^*(p)\hat{b}_p + g_-^*(p)\hat{d}_p) \times \left\{ \iint dp_1 dp_2 v_{p_1}^\dagger(x) v_{p_2}(x) \hat{b}_{p_1}^\dagger(t)\hat{b}_{p_2}(t) + \iint dp_1 dp_2 w_{p_1}^\dagger(x) w_{p_2}(x) \hat{d}_{p_1}^\dagger(t)\hat{d}_{p_2}(t) + \left(\iint dp_1 dp_2 v_{p_1}^\dagger(x) w_{p_2}(x) \hat{b}_p^\dagger(t)\hat{d}_p(t) + \text{H.c.}\right)\right\} \times \int dp(g_+(p)\hat{b}_p^\dagger + g_-(p)\hat{d}_p^\dagger)\|0\rangle\rangle, \tag{13}$$

where H.c. is the conjugate of the preceding term. This density can be parsed as a sum of three terms, each term corresponding to the expectation value obtained for each of the lines given by Eqs. (13),

$$\rho(t,x) = \rho_1(t,x) + \rho_2(t,x) + \rho_3(t,x). \tag{14}$$

$\rho_1(t,x)$ represents a "particle" density, in the sense in which ρ_1 is given only in terms of the positive energy spinor v_p of Eq. (2). The computation is derived by Eqs. (B1)–(B5) of Appendix B. For the same reason, $\rho_2(t,x)$ will be said to represent an "antiparticle" density [it is given by Eq. (B6)], and $\rho_3(t,x)$ represents a "mixed term" [see Eq. (B7)].

Note while ρ_3 only depends on the wave packet (ρ_3 vanishes if there is no wave packet), in the expressions of ρ_1 and ρ_2 there is only a single term that does not depend on the wave packet [the first line in Eqs. (B5) and (B6)]. This term gives the density originating from pair production. Hence, by subsuming these two lines into $\rho_{\text{vac}}(t,x)$, the total density can also be parsed as

$$\rho(t,x) = \rho_{\text{vac}}(t,x) + \rho_{\text{wp}}(t,x), \tag{15}$$

where ρ_{vac} is the "vacuum" particle density (due solely to the background potential) and ρ_{wp} is the part of the density due to the presence of the wave packet.

The total number of particles $N(t) = \int dx\, \rho(t,x)$, obtained by integrating the density over all space, can be parsed as [37]

$$N(t) = \int dx[\rho_1(t,x) + \rho_2(t,x)] = N_{\text{vac}}(t) + 1 \tag{16}$$

given that $\int dx\, \rho_3(x) = 0$ (the wave packet counts as one particle). $N(t)$ can also be written as the normal-ordered expectation value of the number operator $\hat{N}(t)$ written in the standard form

$$\hat{N}(t) = \int dp(\hat{b}_p^\dagger(t)\hat{b}_p(t) + d_p^\dagger(t) d_p(t)). \tag{17}$$

III. MICROCAUSALITY AND THE IMPOSSIBILITY OF SUPERLUMINAL TUNNELING

A. Microcausality with a background field

Microcausality as a general statement is the assertion that observables that are spacelike separated commute. While it may sometimes be considered as an axiom in some versions of QFT [39], microcausality can be explicitly proved for some given quantum fields. In particular, the proof that a noninteracting free Dirac field obeys microcausality is a well-known textbook result [38,40]: if $\hat{O}(t,x)$ and $\hat{O}'(t',x')$ are two observables then

$$[\hat{O}'(t',x'), \hat{O}(t,x)] = 0 \tag{18}$$

for $c^2(t'-t)^2 - (x'-x)^2 < 0$. The standard proof involves writing an arbitrary observable as a bilinear combination of field operators,

$$\hat{O}(t,x) = \hat{\Phi}^\dagger(t,x) o(t,x) \hat{\Phi}(t,x), \tag{19}$$

where $o(t,x)$ is a matrix consisting of c numbers [38,40]. The commutator in Eq. (18) is then written in terms of the anticommutators $[\hat{\Phi}^\dagger(t',x'), \hat{\Phi}(t,x)]_+$. For free Dirac fields, these anticommutators can be computed in closed form [38] and are proved to vanish for spacelike separated intervals. Note that the density operator given by Eq. (9) is the simplest bilinear form involving field operators; this is the only observable we will be interested in in this work.

A straightforward way to verify that microcausality holds here for free Dirac fields is to compute the commutator (18) in a reference frame in which the events are simultaneous, which is always possible (due to Lorentz invariance) for spacelike separated points. In this reference frame the commutator for the density becomes $[\hat{\rho}(t,x), \hat{\rho}(t,y)]$ (with $x \neq y$) which can be readily computed as

$$\begin{aligned}[\hat{\rho}(t,x), \hat{\rho}(t,y)] &= \hat{\Phi}^\dagger(t,x)([\hat{\Phi}(t,x), \hat{\Phi}^\dagger(t,y)]\hat{\Phi}(t,y) \\ &\quad + \hat{\Phi}^\dagger(t,y)[\Phi(\hat{t},x), \hat{\Phi}(t,y)]) \\ &\quad + ([\hat{\Phi}^\dagger(t,x), \hat{\Phi}^\dagger(t,y)]\hat{\Phi}(t,y) \\ &\quad + \hat{\Phi}^\dagger(t,y)[\hat{\Phi}^\dagger(t,x), \hat{\Phi}(t,y)])\hat{\Phi}(t,x) \\ &= \hat{\Phi}^\dagger(t,x)[\hat{\Phi}(t,x), \hat{\Phi}^\dagger(t,y)]_+ \Phi(t,y) \\ &\quad - \hat{\Phi}^\dagger(t,y)[\hat{\Phi}^\dagger(t,x), \hat{\Phi}(t,y)]_+ \hat{\Phi}(t,x) \\ &= 0 \; (x \neq y),\end{aligned} \tag{20}$$

where the last line follows from Eq. (12) involving the equal-time field anticommutators.

It turns out that Eq. (12) also holds for noninteracting Dirac fields in the presence of a background potential. The proof is given in Appendix A [see Eqs. (A5)–(A9)]. Therefore, Eq. (20), the microcausality condition for the density observable, also holds in the presence of a potential barrier. We now hinge on this result to show that the density resulting from tunneling cannot display a superluminal behavior.

B. Microcausality and wave-packet tunneling

We consider the following situation. An electron wave packet is prepared, say to the left of a potential barrier, with its density initially ($t = 0$) localized within a compact support $\mathcal{D}$ defined by $\mathcal{D} = [x_-, x_+]$. Let us label x_0 to be the position of the wave-packet maximum at $t = 0$, and x_+ being the point closest to the barrier. The wave packet is launched towards the barrier; we are interested in the part of the electron density due to the wave packet's dynamical evolution appearing to the right of the barrier density, i.e., the part that has tunneled through the barrier.

Let x' be a point located to the right of the barrier and $\rho(t', x')$ the density at that point. This density is given as per Eq. (8) by the expectation value

$$\rho_\chi(t', x') = \langle\langle \chi \| \hat{\rho}(t', x') \| \chi \rangle\rangle. \quad (21)$$

To be clear ρ_χ represents the full electron density at (t', x') when an initial wave packet is present; the origin of this density can either be due to the wave packet or to the electron and positron pairs created by the potential. Let us now write the density at (t', x') in a different setting, identical to the preceding one except that there is no wave packet at $t = 0$. This density is now given by the vacuum expectation value

$$\rho_0(t', x') = \langle\langle 0 \| \hat{\rho}(t', x') \| 0 \rangle\rangle, \quad (22)$$

and a nonvanishing density can only result from the pair-production process.

Assume (t', x') and $(t = 0, x_+)$ are spacelike separated, implying that (t', x') is spacelike separated from any point of $\mathcal{D}$ over which the wave packet is nonzero at $t = 0$. Let us define the function

$$\mathcal{C}(t', x'; 0, x) = \langle\langle \chi \| \hat{\rho}(t', x') \hat{\rho}(0, x) \| \chi \rangle\rangle, \quad x \in \mathcal{D} \quad (23)$$

correlating an observation of the density at a position x inside the initial wave packet followed by an observation of the density at the spacelike separated point (t', x'). From Eqs. (7) and (10) we obtain, using $\hat{b}_p \hat{b}^\dagger_{p'} \|0\rangle\rangle = \delta(p - p') \|0\rangle\rangle$ and $\hat{d}_p \hat{d}^\dagger_{p'} \|0\rangle\rangle = \delta(p - p') \|0\rangle\rangle$,

$$\begin{aligned} \hat{\Phi}(0, x) \| \chi \rangle\rangle &= \int dp [g_+(p) v_p(x) + g_-(p) w_p(x)] \|0\rangle\rangle \\ &= \chi(0, x) \|0\rangle\rangle. \end{aligned} \quad (24)$$

Similarly we have

$$\langle\langle \chi \| \hat{\Phi}^\dagger(0, x) = \langle\langle 0 \| \chi^\dagger(0, x). \quad (25)$$

We can now write Eq. (23) as

$$\begin{aligned} \mathcal{C}(t', x'; 0, x) &= \langle\langle \chi \| \hat{\rho}(t', x') \hat{\rho}(0, x) \| \chi \rangle\rangle \\ &= \rho_0(t', x') \rho_\chi(0, x), \quad x \in \mathcal{D} \end{aligned} \quad (26)$$

where we have used the definition (9), Eqs. (24) and (25), and the fact that both $\hat{\Phi}^\dagger(t', x')$ and $\hat{\Phi}(t', x')$ anticommute with $\hat{\Phi}(0, x)$ given that the two space-time points $(0, x)$ and (t', x') are spacelike. We have also used Eqs. (21) and (22), writing

$$\rho_\chi(0, x) = \langle\langle \chi \| \hat{\rho}(0, x) \| \chi \rangle\rangle = \chi^\dagger(0, x) \chi(0, x). \quad (27)$$

Equation (26) implies not only that the densities at the two spacelike separated points are independent, but further highlights that the density at (t', x') is a *vacuum* expectation value, that is, it does not depend at all on the wave packet (it can nevertheless be nonzero due to pair production induced by the potential). Equation (26) rules out the possibility of superluminal tunneling because in that case there would be some space-time points (t', x') outside the light cone for which the density at that point would depend on the presence and shape of the wave packet. It is noteworthy that the result (27) does not depend on the shape, width, or height of the background potential. This result holds of course for all types of tunneling: for regular tunneling (characterized by an exponentially decreasing density inside the barrier) or for Klein tunneling (oscillating particle density inside the barrier).

IV. ILLUSTRATIONS

A. Method

We illustrate here our QFT approach by carrying out numerical computations for an electron wave packet, initially localized on a compact support, launched towards a background potential having a rectangularlike shape. We will focus on the transmitted part of the wave packet and consider three typical cases encompassing both standard and Klein tunneling. In the first illustration, we will consider a "low" background potential displaying features similar to the familiar nonrelativistic tunneling case, characterized by a wave packet mostly reflected and transmitted with a very small amplitude. In the second illustration, we will increase the potential barrier, which remains below the supercriticial threshold ($2mc^2$) but is already sufficient in order to visualize the nontrivial interplay between the transmitted wave packet and the exponentially small electron density due to pair production. In the third illustration, we will consider a backround potential lying in the supercritical regime, with a wave-packet energy giving rise to Klein tunneling: the density oscillates inside the barrier and the wave packet is transmitted with a very high amplitude.

To be specific, we will deal in all cases with an initial wave packet given by the Dirac spinor

$$G(x) = \left[\cos^8\left(\frac{x - x_0}{D}\right) e^{ip_0 x}, 0\right] [\theta(x - x_-) - \theta(x - x_+)] \quad (28)$$

defined to be nonzero only over the compact support $x \in \mathcal{D}$ (θ is the units step function). $\mathcal{D}$ is defined by $\mathcal{D} = [x_-, x_+]$ with $x_\pm = x_0 \pm D\pi/2$ and is localized to the left of the barrier (πD is the length of the support and x_0 is the position of the maximum of the wave packet). The $\cos^8$ function was chosen for computational convenience; p_0 is the initial mean momentum. p_0 and D are chosen such that the electron wave packet moves towards the right as time evolves and the entire wave packet remains below the potential threshold. By projecting $G(x)$ over the free Dirac basis $v_p(x)$ and $w_p(x)$ we obtain the coefficients $g_\pm(p)$ of Eq. (7) defining the initial second-quantized wave packet[1] which is in turn fed in Eq. (8) in order to obtain the space-time resolved density $\rho(t, x)$.

To this end we need to compute the unitary evolution elements appearing in the density expressions [see Eqs. (B5)–(B7)], such as $U_{v_k w_p}(t)$ given by Eq. (4). The background potential is set to be

$$V(x) = \frac{V_0}{2} \{\tanh[(x + L/2)/\epsilon] - \tanh[(x - L/2)/\epsilon]\}, \quad (29)$$

where V_0 and L are the barrier height and width, respectively, and ϵ a smoothness parameter. We then determine the evolution operator by solving the corresponding Dirac equation on a

[1]Recall that the first-quantized wave packet is obtained from the Fock space state through $\chi(t, x) = \langle\langle 0 \| \hat{\Phi}(t, x) \| \chi \rangle\rangle$ [37,41].

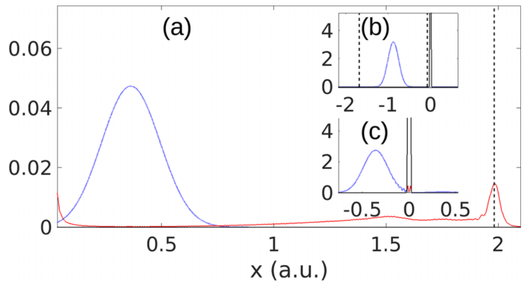

FIG. 1. Space-time resolved densities for the case 1 tunneling wave packet. (a) The density of the transmitted wave packet is shown (dotted blue) as it is exiting the barrier ($t = 1.5 \times 10^{-2}$ a.u.) for a comparatively low potential ($V_0 = 0.5mc^2$) giving rise to standard tunneling, with a negligible pair creation rate (the electron density created by the potential is shown in red). The inset displays snapshots of the wave-packet dynamics at (b) $t = 0$ and at (c) $t = 1.5 \times 10^{-2}$ a.u [note the transmitted wave packet is hardly visible on that scale in (c)]. The dotted vertical line in (b) represents the right edge of the support $\mathcal{D}$ over which the initial wave packet is defined. The same line in (a) and (c) represents the position of the light cone emanating from this right edge at the time of the plot. The initial wave-packet parameters in atomic units (a.u.) are $x_0 = -120\lambda$, $p_0 = 100$ a.u., and $\mathcal{D} = 70\lambda$ and for the barrier $L = 4\lambda$ and $\varepsilon = 0.3\lambda$, where $\lambda = \hbar/mc$ is the Compton wavelength of the electron.

discretized space-time grid using a split operator [42] method (the evolution operator is split into a kinetic part propagated in momentum space and a potential-dependent part solved in position space). Note that in order to simplify the numerics we have chosen $t = 0$ as the time the barrier is raised and starts radiating and also as the time the wave packet is launched (although these two starting times are independent).

B. Standard tunneling

1. Case 1

Figure 1 shows the transmitted wave packet as well as the electron density due to pair production for a comparatively "low" potential ($V_0 = 0.5mc^2$). Snapshots of the density evolution are given in the inset; leaving aside pair production, this situation is a QFT account of the familiar Schrödinger-type tunneling dynamics, where most of the incoming electron amplitude is reflected and only a very small amplitude is transmitted.

Note that the light cone (emanating from the space-time point $t = 0,\ x = x_+$) lies far ahead of the transmitted wave packet. Indeed, although the wave packet is ultrarelativistic ($p_0 = 100$ a.u.) the mean velocity, roughly estimated as $u \simeq pc/\sqrt{p^2 + m^2c^2} = 0.59c$, is still far from c. A computation of the momentum distribution of the initial state shows that coefficients $|g_+(p)|$ with $p > p_0 + 20$ a.u. become vanishingly small and do not contribute to the wave packet, while any contribution with $p > 153.2$ a.u. would go over the barrier and would therefore not tunnel.

2. Case 2

Figure 2 shows the situation for a higher barrier ($V_0 = 1.77mc^2$) at $t_p = 3 \times 10^{-3}$ a.u. Pair production is still small, as the total number of electrons due to pair production is $N_{\mathrm{vac}}(t_p)/2 = 0.31$ [see Eq. (16)], but the transmitted wave-packet amplitude is even smaller. As a result, the transmitted wave packet appears as a small bump in the overall density (red line in Fig. 2). This is confirmed by applying Eq. (15) that allows for the computation of the part of the density due to the wave packet (blue line in Fig. 2). Note that some of the works [17–25] investigating relativistic tunneling within the first-quantized approximation have computed numerical results for barrier heights in cases in which QFT calculations show that the tiny amplitude of the transmitted wave packet would be completely overshadowed by the larger (or much larger if supercritical barriers are considered) electron density produced by the barrier.

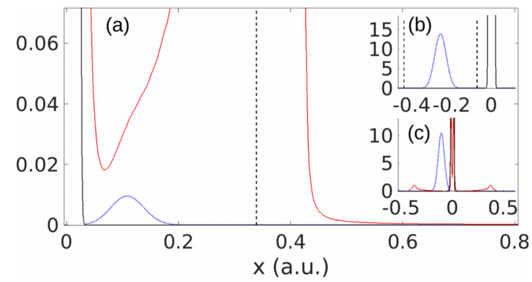

FIG. 2. Numerical computations corresponding to case 2, i.e., standard tunneling with a slightly radiating potential $V_0 = 1.77mc^2$. (a) The *total* density of the transmitted wave packet is shown in red. The transmitted wave packet is barely visible as a bump in the total density, although calculations show the wave-packet density (dotted blue). The inset displays snapshots of the wave-packet dynamics at (b) $t = 0$ and at (c) $t = 3 \times 10^{-3}$ [the time of the plot (a)]. The initial wave-packet parameters are (in a.u.) $x_0 = -35\lambda$, $p_0 = 200$, and $\mathcal{D} = 16\lambda$ and for the barrier $L = 4\lambda$ and $\varepsilon = 0.3\lambda$, where $\lambda = \hbar/mc$.

Figure 2 also shows the light cone, emanating from the right edge x_+ of the initial wave-packet density distribution; it can be seen that although the electron is in the relativistic regime (the mean velocity of the initial distribution is $0.83c$), the transmitted wave packet remains well inside the light cone, in line with the results of Sec. III.

C. Klein tunneling

Klein tunneling takes place for supercritical potentials ($V_0 > 2mc^2$) and wave-packet energies for which $(E - V_0)^2 > m^2c^4$; in this case the transmission of the electron wave packet is mediated by pair production [31,43] giving rise to an oscillating density inside the barrier. These modulations in pair production give rise to a transmitted wave packet with an undamped amplitude (as opposed to an exponentially decreasing transmission in the case of regular tunneling). Relative to the freely propagated wave packet, the transmitted Klein tunneled one can be accelerated by the barrier (since the negative energy wave-packet components see a potential well [44]) but never faster than light since our result (26) holds for any type of potential barrier. A computation illustrating Klein tunneling is given in Fig. 3, for $V_0 = 9mc^2$.

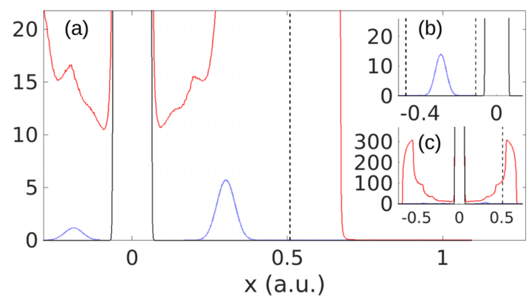

FIG. 3. Numerical results for case 3 (Klein tunneling), with a supercritical barrier of height $V_0 = 9mc^2$. (a) The electron wave-packet density is shown (dotted blue) at $t = 4.5 \times 10^{-3}$ a.u. well after the transmitted wave packet (centered at $x \approx 0.3$ a.u.) has exited the barrier (solid vertical lines). Note that the transmitted wave-packet density is significantly larger than the one of the reflected wave packet (centered at $x = -0.19$ a.u. and moving toward the left). (b) The initial wave packet (light blue) is shown along with the support $\mathcal{D}$ (dashed lines) and the barrier. (c) The plot (a) is zoomed out in order to visualize the electron density due to pair production (red line). The wave packet is not visible at this scale. The initial wave-packet parameters in a.u. are $x_0 = -40\lambda$, $p_0 = 450$ a.u., and $\mathcal{D} = 16\lambda$ and for the barrier $L = 16\lambda$ and $\varepsilon = 0.3\lambda$ with $\lambda = \hbar/mc$.

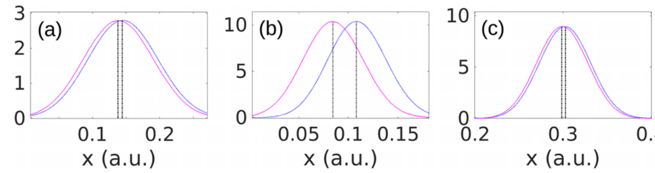

FIG. 4. (a)–(c) Display for each case considered, respectively, in Figs. 1–3 the position of the transmitted peak along with the position of the same initial wave packet that would have evolved freely. The vertical dotted lines indicate the maxima of the transmitted peak and the free wave packets (see text for details).

V. DISCUSSION AND CONCLUSION

Although we have shown in Sec. III that according to our space-time resolved relativistic QFT framework to spin-$\frac{1}{2}$ fermions there can be no superluminality in tunneling transmission, it is often asserted that tunneling can be superluminal or instantaneous. It is worthwhile briefly recalling on which grounds such assertions have been made.

First, we must discard models based on nonrelativistic frameworks, like the Schrödinger equation, for which propagation is indeed instantaneous [45]. The same holds for semiclassical approaches based on the Schrödinger equation. Experimental results, in particular those involving the attoclock technique in strong field ionization (see, e.g., [2,5,10,11]), have usually relied on such models when estimating tunneling times. Superluminality appears here as an artifact of employing a nonrelativistic approach.

Second, there is the problem of defining traversal times during the tunneling process. Indeed, there is no unambiguous manner to define a tunneling time [15]. Various candidates have been proposed (phase delays, dwell times, Larmor times, time operators, weak values). These quantities not only lead to conflicting results (predicting strikingly different traversal times) but furthermore by construction they can yield superluminal values, including when they are employed with relativistic wave equations [17,19–21,23,25].

Third, some first-quantized works based on relativistic wave equations have suggested superluminal transmission based on the fact that the maximum of the density (or of the current density) of the transmitted wave packet arrives earlier than the maximum of the freely propagating one [18,23,24]. We note that in the three numerical cases given in Sec. IV we can also observe the same phenomenon: as illustrated in Fig. 4 the maximum of the tunneled wave packet has traveled, at a given time, a longer distance than the maximum of an initially identical wave packet that would have evolved freely. This is of course compatible with the causal dynamics implied by Eq. (26). Indeed, having the maximum of a peak appearing earlier at a given position does not imply faster or superluminal dynamics: the important point is that the "advanced" peak still lies within the envelope of the free wave packet.

Note that even within first-quantized quantum mechanics it would be incorrect to associate part of the quantum state (the transmitted wave packet) with a single particle somehow emerging faster from the barrier. Such a view would be clearly incompatible with a QFT based framework. According to QFT, a particle at each space-time point of a wave packet is seen as a field excitation at that particular point, and the field excitation at that point can only be related causally to the field excitation at some other space-time point, in particular to the field excitation at a different position in a given reference frame. Put differently, the causality implied by Eq. (26) only imposes that the field excitation at the maximum of the transmitted wave packet must lie within the forward light cone emanating from $\mathcal{D}$.

To sum up, we have investigated the tunneling wave-packet dynamics for an electron within a relativistic QFT framework in which the barrier is modeled as a background field. We have shown that if the electron wave packet is initially ($t = 0$) localized to the left of the barrier, the electron density at a spacelike separated point to the right of the barrier does not depend on the presence or absence of the wave packet at $t = 0$, thereby precluding any superluminal effects related to tunneling. We have numerically computed the space-time resolved electron density in typical cases of tunneling with potentials below, close to or above the supercritical value. We hope our results will contribute in clarifying the models and approximations employed when accounting for results involving traversal or detection times in tunneling related effects. We can expect similar results to hold for other types of relativistic quantum fields known to obey microcausality.

ACKNOWLEDGMENTS

We are grateful for Grant No. PID2021-126273NB-I00, funded by MCIN/AEI/10.13039/ 501100011033 and "ERDF A way of making Europe." We acknowledge financial support from the Basque Government, Grant No. IT1470-22. M.P. acknowledges financial support from the Spanish MICIN, Grant No. PID2022-141283NB-100.

APPENDIX A: FIELD OPERATORS: EQUAL-TIME ANTICOMMUTATORS

We prove here the equal-time anticommutator given by Eq. (12) with the field operator $\hat{\Phi}(t,x)$ given in terms of the annihilation operators of particles and antiparticles by Eq. (10).

1. Field-free case

In the *field-free* case, the time evolution of the creation and annihilation operators is trivial $[\hat{b}_p(t) = e^{iE_pt}\hat{b}_p,\ \hat{d}_p^\dagger(t) = e^{-iE_{p'}t}\hat{d}_p^\dagger$, etc.] and the equal-time anticommutator reads as

$$[\hat{\Phi}^\dagger(x), \hat{\Phi}(y)]_+ = \left[\int dp\, \hat{b}_p^\dagger v_p^\dagger(x)e^{iE_pt} + \int dp\, \hat{d}_p^\dagger w_p^\dagger(x)e^{-iE_pt},\ \int dp' \hat{b}_{p'} v_{p'}(y)e^{-iE_{p'}t} + \int dp\, \hat{d}_{p'} w_{p'}(y)e^{-iE_{p'}t}\right]_+. \tag{A1}$$

Using the anticommutation relations

$$[\hat{b}_p^\dagger, \hat{b}_{p'}]_+ = [\hat{d}_p^\dagger, \hat{d}_{p'}]_+ = \delta(p-p'),$$
$$[\hat{b}_p^\dagger, \hat{d}_{p'}]_+ = [\hat{d}_p^\dagger, \hat{b}_{p'}]_+ = \delta(p-p') \tag{A2}$$

and

$$v_p^\dagger(x)v_p(y) = e^{ip(y-x)},$$
$$w_p^\dagger(x)w_p(y) = e^{-ip(x-y)}, \tag{A3}$$

we obtain

$$[\hat{\Phi}^\dagger(x), \hat{\Phi}(y)]_+ = \int dp(e^{ip(y-x)} + e^{ip(x-y)}) \tag{A4}$$

which leads to Eq. (12) of the paper.

2. Background potential

In the presence of a *background potential*, the equal-time anticommutation relation

$$[\hat{\Phi}^\dagger(t,x), \hat{\Phi}(t,y)]_+ = \left[\int dp(\hat{b}_p^\dagger(t)v_p^\dagger(x) + \hat{d}_p^\dagger(t)w_p(x)^\dagger),\ \int dp(\hat{b}_p(t)v_p(x) + \hat{d}_p(t)w_p(x))\right]_+ \tag{A5}$$

involves the anticommutators of the type

$$\left[\hat{b}_{p_1}^\dagger(t), b_{p_2}(t)\right] = \left[\int dp_1'\big(U^*_{v_{p_1}w_{p_1'}}\hat{b}^\dagger_{p_1'} + U^*_{v_{p_1}w_{p_1'}}\hat{d}_{p_1'}\big),\ \int dp_2'\big(U_{v_{p_2}v_{p_2'}}\hat{b}_{p_2'} + U_{v_{p_2}w_{p_2'}}\hat{d}^\dagger_{p_2'}\big)\right]_+. \tag{A6}$$

Using Eq. (5) of the main text, one obtains

$$\begin{aligned}\left[\hat{b}_{p_1}^\dagger(t), b_{p_2}(t)\right]_+ &= \int d_{p_1'}\big(U^*_{v_{p_1}v_{p_1'}}U_{v_{p_2}v_{p_1'}} + U^*_{v_{p_1}w_{p_1'}}U_{v_{p_2}w_{p_1'}}\big)\\ &= \int d_{p_1'}\big(\langle v_{p_2}|\hat{U}|v_{p_1'}\rangle\langle v_{p_1'}|\hat{U}^\dagger|v_{p_1}\rangle\\ &\quad+\langle v_{p_2}|\hat{U}|w_{p_1'}\rangle\langle w_{p_1'}|\hat{U}^\dagger|v_{p_1}\rangle\big)\\ &= \langle v_{p_2}|\hat{U}\hat{U}^\dagger|v_{p_1}\rangle = \langle v_{p_2}|v_{p_1}\rangle = \delta(p_1-p_2),\end{aligned} \tag{A7}$$

where in the last line we used the completeness relation

$$\int dp'(|v_{p'}\rangle\langle v_{p'}| + |w_{p'}\rangle\langle w_{p'}|) = 1$$

and the orthonormality of the solutions of the free Dirac equation. Similarly, we find that

$$\left[\hat{d}_{p_1}^\dagger(t), d_{p_2}(t)\right]_+ = \delta(p_1-p_2). \tag{A8}$$

Plugging- these anticommutators into Eq. (A5) leads to

$$[\hat{\Phi}^\dagger(t,x), \hat{\Phi}(t,y)]_+ = \int dp(e^{ip(y-x)} + e^{ip(x-y)}) \tag{A9}$$

and hence again to Eq. (12) of the paper.

APPENDIX B: DERIVATION OF THE DENSITY EXPRESSIONS

We derive here the expression of the particle density, given by Eq. (8) which becomes Eq. (14). Let us first compute the expectation value of the operator written in Eq. (13), written as

$$\rho_1(t,x) = \langle\langle 0\| \int dp(g_+^*(p)\hat{b}_p + g_-^*(p)\hat{d}_p)\left\{\iint dp_1dp_2 v_{p_1}^\dagger(x)v_{p_2}(x)\int dp'\big(U^*_{v_{p_1}v_{p'}}(t)\hat{b}^\dagger_{p'} + U^*_{v_{p_1}w_{p'}}(t)\hat{d}_{p'}\big)\int dp'\big(U_{v_{p_2}v_{p'}}(t)\hat{b}_{p'} + U_{v_{p_2}w_{p'}}(t)\hat{d}^\dagger_{p'}\big)\right\}\int dp\big(g_+(p)\hat{b}_p^\dagger + g_-(p)\hat{d}_p^\dagger\big)\|0\rangle\rangle \tag{B1}$$

which expands to

$$\begin{aligned}\rho_1(t,x) = &\langle\langle 0\|\int\cdots\int dq_1dq_1'dq_2dq_2'dp_1dp_2 g_-^*(q_1)g_-(q_2)U^*_{v_{p_1}w_{q_1'}}(t)U_{v_{p_2}w_{q_2'}}(t)v_{p_1}^\dagger(x)\Phi_{p_2}(x)\hat{d}_{q_1}\hat{d}_{q_1'}\hat{d}^\dagger_{q_2'}\hat{d}^\dagger_{q_2}\|0\rangle\rangle\\ &+\langle\langle 0\|\int\cdots\int dq_1dq_1'dq_2dq_2'dp_1dp_2 g_+^*(q_1)g_+(q_2)U^*_{v_{p_1}w_{q_1'}}(t)U_{v_{p_2}w_{q_2'}}(t)v_{p_1}^\dagger(x)v_{p_2}(x)\hat{b}_{q_1}\hat{d}_{q_1'}\hat{d}^\dagger_{q_2'}\hat{b}^\dagger_{q_2}\|0\rangle\rangle\\ &+\langle\langle 0\|\int\cdots\int dq_1dq_1'dq_2dq_2'dp_1dp_2 g_+^*(q_1)g_+(q_2)U^*_{v_{p_1}v_{q_1'}}(t)U_{v_{p_2}v_{q_2'}}(t)v_{p_1}^\dagger(x)v_{p_2}(x)\hat{b}_{q_1}\hat{b}^\dagger_{q_1'}\hat{b}_{q_2'}\hat{b}^\dagger_{q_2}\|0\rangle\rangle.\end{aligned} \tag{B2}$$

Using the anticommutation relations of creation and annihilation operators

$$\langle\langle 0\|\hat{d}_{q_1}\hat{d}_{q_1'}\hat{d}^{\dagger}_{q_2'}\hat{d}^{\dagger}_{q_2}\|0\rangle\rangle = \delta_{q_1'q_2'}\delta_{q_1q_2} - \delta_{q_1q_2'}\delta_{q_1'q_2},$$
$$\langle\langle 0\|\hat{b}_{q_1}\hat{d}_{q_1'}\hat{d}^{\dagger}_{q_2'}\hat{b}^{\dagger}_{q_2}\|0\rangle\rangle = \delta_{q_1q_2}\delta_{q_1'q_2'},$$
$$\langle\langle 0\|\hat{b}_{q_1}\hat{b}^{\dagger}_{q_1'}\hat{b}_{q_2'}\hat{b}^{\dagger}_{q_2}\|0\rangle\rangle = \delta_{q_1q_2'}\delta_{q_2q_2'}, \tag{B3}$$

we get

$$\begin{aligned}\rho_1(t,x) = &\int dq|g_-(q)|^2\int dq\left(\int U_{v_pw_q}(t)v_p(x)\right)^{\dagger}\left(\int U_{v_pw_q}(t)v_p(x)\right)\\ &+\int dq|g_+(q)|^2\int dq\left(\int U_{v_pw_q}(t)v_p(x)\right)^{\dagger}\left(\int U_{v_pw_q}(t)v_p(x)\right)\\ &+\left(\int dp\,dq\,g_+(p)U_{v_pv_q}v_p(x)\right)^{\dagger}\left(\int dp\,dq\,g_+(p)U_{v_pv_q}v_p(x)\right)\\ &-\left(\int dp\,dq\,g_-(p)U_{v_pw_q}v_p(x)\right)^{\dagger}\left(\int dp\,dq\,g_-(p)U_{v_pw_q}v_p(x)\right).\end{aligned} \tag{B4}$$

Using the normalization of the initial QFT state yields

$$\begin{aligned}\rho_1(t,x) = &\int dq\left(\int U_{v_pw_q}(t)v_p(x)\right)^{\dagger}\left(\int U_{v_pw_q}(t)v_p(x)\right)\\ &+\left(\int dp\,dq\,g_+(p)U_{v_pv_q}(t)v_p(x)\right)^{\dagger}\left(\int dp\,dq\,g_+(p)U_{v_pv_q}(t)v_p(x)\right)\\ &-\left(\int dp\,dq\,g_-(p)U_{v_pw_q}(t)v_p(x)\right)^{\dagger}\left(\int dp\,dq\,g_-(p)U_{v_pw_q}(t)v_p(x)\right).\end{aligned} \tag{B5}$$

The first line in the expression of $\rho_1(t,x)$ represents the electron density created by the background potential due to the vacuum excitation while the second line represents the density corresponding to the incoming particle. The third line represents the modulation in the number density of the created particles due to the incident particle wave packet. The terms $\rho_2(t,x)$ and $\rho_3(t,x)$ are computed similarly, yielding

$$\begin{aligned}\rho_2(t,x) = &\int dp\left(\int dq\,U_{w_pv_q}(t)w_p(x)\right)^{\dagger}\left(\int dq\,U_{w_pv_q}(t)w_p(x)\right)\\ &+\left(\int dp\,dq\,g_-(q)U_{w_pw_q}(t)w_p(x)\right)^{\dagger}\left(\int dp\,dq\,g_-(q)U_{w_pw_q}(t)w_p(x)\right)\\ &-\left(\int dp\,dq\,g_+(q)U_{w_qw_p}(t)w_p(x)\right)^{\dagger}\left(\int dp\,dq\,g_+(q)U_{w_qv_q}(t)w_p(x)\right)\end{aligned} \tag{B6}$$

and

$$\begin{aligned}\rho_3(t,x) = &\,2\,\mathrm{Re}\left(\int dp\,dq\,g^*_-(q)U^*_{w_pw_q}(t)g_+(q)U_{v_pv_q}w^{\dagger}_q(x)v_p(x)\right)\\ &+2\,\mathrm{Re}\left(\int dp\,dq\,g^*_-(q)U^*_{w_pv_q}(t)g_+(q)U_{v_pw_q}w^{\dagger}_q(x)v_p(x)\right),\end{aligned} \tag{B7}$$

where $\rho_2(t,x)$ is the counterpart of $\rho_1(t,x)$ for the positron density while $\rho_3(t,x)$ involves cross terms between positive and negative energy modes of the initial wave packet. $\rho_3(t,x)$ cancels the infinite tails of $\rho_1(t,x)$ and $\rho_2(t,x)$. When integrated over the entire space, however, the contribution of this term vanishes, ensuring that ρ obeys

$$\int dx\,\rho(t,x) = \int dx\,\rho_1(t,x) + \int dx\,\rho_2(t,x), \tag{B8}$$

which is the sum of the particle and antiparticle numbers.

[1] M. Garg and K. Kern, Attosecond coherent manipulation of electrons in tunneling microscopy, Science **367**, 411 (2020).
[2] U. S. Sainadh, H. Xu, X. Wang, A. Atia-Tul-Noor, W. C. Wallace, N. Douguet, A. Bray, I. Ivanov, K. Bartschat, A. Kheifets, R. T. Sang, and I. V. Litvinyuk, Attosecond angular streaking and tunnelling time in atomic hydrogen, Nature (London) **568**, 75 (2019).
[3] D. C. Spierings and A. M. Steinberg, Observation of the decrease of Larmor tunneling times with lower incident energy, Phys. Rev. Lett. **127**, 133001 (2021).
[4] Z. Guo, Y. Fang, P. Ge, X. Yu, J. Wang, Meng Han, Q. Gong, and Y. Liu, Probing tunneling dynamics of dissociative H_2 molecules using two-color bicircularly polarized fields, Phys. Rev. A **104**, L051101 (2021).
[5] M. Yu, K. Liu, M. Li, J. Yan, C. Cao, J. Tan, J. Liang, K. Guo, W. Cao, P. Lan *et al.*, Full experimental determination of tunneling time with attosecond-scale streaking method, Light Sci. Appl. **11**, 215 (2022).
[6] Y. K. Lee, H. Lin, and W. Ketterle, Spin dynamics dominated by resonant tunneling into molecular states, Phys. Rev. Lett. **131**, 213001 (2023).
[7] M. M. Elahi, H. Vakili, Y. Zeng, C. R. Dean, and A. W. Ghosh, Direct evidence of Klein and anti-Klein tunneling of graphitic electrons in a Corbino geometry, Phys. Rev. Lett. **132**, 146302 (2024).
[8] J. G. Muga and C. R. Leavens, Arrival time in quantum mechanics, Phys. Rep. **338**, 353 (2000).
[9] U. S. Sainadh, R. T. Sang and I. V. Litvinyuk, Attoclock and the quest for tunnelling time in strong-field physics, J. Phys. Photon. **2**, 042002 (2020).
[10] P. Eckle, A. N. Pfeiffer, C. Cirelli, A. Staudte, R. Dörner, H. G. Muller, M. Büttiker, and U. Keller, Attosecond ionization and tunneling delay time measurements in helium, Science **322**, 1525 (2008).
[11] A. N. Pfeiffer, C. Cirelli, M. Smolarski, D. Dimitrovski, M. Abu-samha, L. B. Madsen, and U. Keller, Attoclock reveals natural coordinates of the laser-induced tunnelling current flow in atoms, Nat. Phys. **8**, 76 (2012).
[12] T. Zimmermann, S. Mishra, B. R. Doran, D. F. Gordon, and A. S. Landsman, Tunneling time and weak measurement in strong field ionization, Phys. Rev. Lett. **116**, 233603 (2016).
[13] M. Hino, N. Achiwa, S. Tasaki, T. Ebisawa, T. Kawai, T. Akiyoshi, and D. Yamazaki, Measurement of Larmor precession angles of tunneling neutrons, Phys. Rev. A **59**, 2261 (1999).
[14] P. Fevrier and J. Gabelli, Tunneling time probed by quantum shot noise, Nat. Commun. **9**, 4940 (2018).
[15] D. Sokolovski and E. Akhmatskaya, No time at the end of the tunnel, Commun. Phys. **1**, 47 (2018).
[16] M. Klaiber, Q. Z. Lv, S. Sukiasyan, D. Bakucz Canario, K. Z. Hatsagortsyan, and C. H. Keitel, Reconciling conflicting approaches for the tunneling time delay in strong field ionization, Phys. Rev. Lett. **129**, 203201 (2022).
[17] P. Krekora, Q. Su, and R. Grobe, Effects of relativity on the time-resolved tunneling of electron wave packets, Phys. Rev. A **63**, 032107 (2001).
[18] V. Petrillo and D. Janner, Relativistic analysis of a wave packet interacting with a quantum-mechanical barrier, Phys. Rev. A **67**, 012110 (2003).
[19] H. G. Winful, M. Ngom, and N. M. Litchinitser, Relation between quantum tunneling times for relativistic particles, Phys. Rev. A **70**, 052112 (2004); **108**, 019902(E) (2023).
[20] S. De Leo and P. P. Rotelli, Dirac equation studies in the tunneling energy zone, Eur. Phys. J. C **51**, 241 (2007).
[21] A. E. Bernardini, Delay time computation for relativistic tunneling particles, Eur. Phys. J. C **55**, 125 (2008).
[22] O. del Barco and V. Gasparian, Relativistic tunnelling time for electronic wave packets, J. Phys. A: Math. Theor. **44**, 015303 (2011).
[23] S. De Leo, A study of transit times in Dirac tunneling, J. Phys. A: Math. Theor. **46**, 155306 (2013).
[24] R. S. Dumont, T. Rivlin, and E. Pollak, The relativistic tunneling flight time may be superluminal, but it does not imply superluminal signaling, New J. Phys. **22**, 093060 (2020).
[25] P. C. Flores and E. A. Galapon, Instantaneous tunneling of relativistic massive spin-0 particles, Europhys. Lett. **141**, 10001 (2023).
[26] J. C. Park and Y. J. Lee, Superluminality and causality in the relativistic barrier problem, J. Korean Phys. Soc. **43**, 4 (2003).
[27] C. Anastopoulos and N. Savvidou, Quantum temporal probabilities in tunneling systems, Ann. Phys. **336**, 281 (2013).
[28] M. Alkhateeb, X. G. de la Cal, M. Pons, D. Sokolovski and A. Matzkin, Relativistic time-dependent quantum dynamics across supercritical barriers for Klein-Gordon and Dirac particles, Phys. Rev. A **103**, 042203 (2021).
[29] L. Gavassino and M. M. Disconzi, Subluminality of relativistic quantum tunneling, Phys. Rev. A **107**, 032209 (2023).
[30] T. Cheng, Q. Su, and R. Grobe, Introductory review on quantum field theory with space–time resolution, Contemp. Phys. **51**, 315 (2010).
[31] M. Alkhateeb and A. Matzkin, Space-time-resolved quantum field approach to Klein-tunneling dynamics across a finite barrier, Phys. Rev. A **106**, L060202 (2022).
[32] J. Unger, S. Dong, Q. Su, and R. Grobe, Optimal supercritical potentials for the electron-positron pair-creation rate, Phys. Rev. A **100**, 012518 (2019).
[33] D. D. Su, Y. T. Li, Q. Z. Lv, and J. Zhang, Enhancement of pair creation due to locality in bound-continuum interactions, Phys. Rev. D **101**, 054501 (2020).
[34] S. P. Gavrilov and D. M. Gitman, Consistency restrictions on maximal electric-field strength in quantum field theory, Phys. Rev. Lett. **101**, 130403 (2008).
[35] H. Feschbach and F. Villars, Elementary relativistic wave mechanics of spin 0 and spin 1/2 particles, Rev. Mod. Phys. **30**, 24 (1958).
[36] S. A. Fulling, *Aspects of Quantum Field Theory in Curved Spacetime* (Cambridge University Press, Cambridge, Great Britain, 1989).
[37] M. Alkhateeb and A. Matzkin, Evolution of strictly localized states in noninteracting quantum field theories with background fields, Phys. Rev. A **109**, 062223 (2024).
[38] W. Greiner, *Field Quantization* (Springer, Berlin, 1996).
[39] C. J. Fewster and K. Rejzner, Algebraic Quantum Field Theory? An introduction, in *Progress and Visions in Quantum Theory in View of Gravity*, edited by F. Finster *et al.* (Springer, Berlin, 2020).

[40] T. Padmanabhan, *Quantum Field Theory* (Springer, Switzerland, 2016).
[41] S. S. Schweber, *An Introduction to Relativistic Quantum Field Theory* (Dover, New York, 2005).
[42] M. Ruf, H. Bauke, and C. H. Keitel, A real space split operator method for the Klein–Gordon equation, J. Comput. Phys. **228**, 9092 (2009).
[43] P. Krekora, Q. Su, and R. Grobe, Klein paradox in spatial and temporal resolution, Phys. Rev. Lett. **92**, 040406 (2004).
[44] N. Dombey and A. Calogeracos, Seventy years of the Klein paradox, Phys. Rep. **315**, 41 (1999).
[45] G. C. Hegerfeldt and S. N. M. Ruijsenaars, Remarks on causality, localization, and spreading of wave packets, Phys. Rev. D **22**, 377 (1980).